Project 079 Novel Noise Liner Development Enabled by Advanced Manufacturing

The Pennsylvania State University

Project Lead Investigator

Timothy W. Simpson
Paul Morrow Professor of Engineering Design & Manufacturing
Department of Mechanical Engineering
The Pennsylvania State University
University Park, PA 16803
814-863-7136
tws8@psu.edu

University Participants

The Pennsylvania State University

- P.I.: Timothy W. Simpson, Paul Morrow Professor of Engineering Design & Manufacturing
- FAA Award Number: 13-C-AJFE-PSU-079
- Period of Performance: October 1, 2021 to September 30, 2022 (no cost extension to December 31, 2022)
- Tasks:
    1. Preliminary design and acoustic analysis of novel liners for testing
    2. Detailed design and additive fabrication of novel liner solutions
    3. Acoustic evaluation of additively manufactured novel liners

Project Funding Level

$300,000 from FAA; $300,000 match from The Pennsylvania State University ($100,000) and Raytheon Technologies Research Center ($200,000)

Investigation Team

The Pennsylvania State University (PSU):

- Tim Simpson, P.I., responsible for project management, task coordination, and student advising
- Allison Beese, co-P.I., responsible for supporting Task 1 and student advising
- Eric Greenwood, co-P.I., responsible for supporting Task 3 and student advising
- Jay D. Martin, co-P.I., responsible for supporting Task 2 and student co-advising
- Andy Swanson, graduate student (MS), responsible for work on Tasks 1–3
- Michael Geuy, graduate student (PhD), responsible for work on Tasks 1–3

Raytheon Technologies Research Center (RTRC):

- Jeff Mendoza, P.I., responsible for project coordination and management at RTRC
- Julian Winkler, co-P.I., responsible for acoustic analysis and evaluation as part of Tasks 1–3
- Aaron Reimann, co-P.I., responsible for acoustic analysis and evaluation as part of Tasks 1–3
- Kenji Homma, co-P.I., responsible for acoustic analysis and evaluation as part of Tasks 1–3
- Paul Braunwart, co-P.I., responsible for acoustic analysis and evaluation as part of Tasks 1–3

Project Overview

PSU and its Applied Research Laboratory in collaboration with its industrial partner, RTRC, and government collaborator, NASA Langley Research Center (LaRC), are helping the FAA develop and advance innovative engine acoustic liner technology to meet the demands of low noise for future aircraft. The team is developing and demonstrating a methodology to design and manufacture novel lattice structures that enhance noise attenuation in aircraft engines. Analysis and experimental testing are applied to understand the effect of geometry and feature size of the lattices to control noise while ensuring the manufacturability of these complex structures in different materials. Advanced manufacturing technologies are used to enable rapid design–build–test cycles for design development, including assessments of structural integrity and acoustic performance. Promising engine liner designs and their performance will be documented and archived for the FAA to aid future advancements in aircraft engine noise reduction.

The overall project approach includes the following steps:

1. Establish a set of acoustic requirements for future aircraft engine designs.
2. Design and analyze lattice-based acoustic liners using advanced software tools.
3. Perform rapid, iterative prototyping and testing to identify promising designs and materials.
4. Conduct detailed assessments of manufacturability.
5. Perform acoustic and structural evaluations of novel liners in collaboration with NASA LaRC.
6. Document results and archive data for the FAA.

This project will be accomplished through the three tasks described below.

Task 1 - Preliminary Design and Acoustic Analysis of Novel Liners

PSU and RTRC contributed to this task.

Objective

The goal of Task 1 is to develop and demonstrate a methodology for rapid design, analysis, fabrication, and testing of novel structures that can enhance noise attenuation in aircraft engines.

Research Approach

Design framework

The team prototyped a digital workflow to design, analyze, fabricate, and test acoustic liner geometries in Year 1 by using the different additive manufacturing (AM) capabilities available at PSU's Center for Innovative Materials Processing through Direct Digital Deposition and leveraging the liner acoustic performance prediction capabilities developed at RTRC. The rapid acoustic liner development methodology is illustrated in Figure 1, color-coded based on who is primarily responsible for each aspect of the framework. As indicated, the PSU and RTRC teams are working together to generate solid models of acoustic liners, which are then exported for analysis and manufacturing. PSU (in blue) selects a suitable AM process and material, plans and fabricates the liner, and then post-processes the liner prior to inspection. In parallel, RTRC (in salmon) performs simulations at varying levels of fidelity based on the level of analysis desired. Reduced-order models give rapid, but less accurate results, while finite element (FE) methods and the lattice Boltzmann method (LBM) provide increased accuracy at higher computational cost. Metrics of interest are predicted and then compared with appropriate test results from normal impedance tube (NIT) testing (at PSU, RTRC, and NASA LaRC) and grazing flow impedance tube (GFIT) testing (at RTRC and NASA LaRC). Results are then collected, stored, and reviewed by all to identify the next design iteration.

The multi-fidelity approach developed and used at RTRC to expedite acoustic analysis is shown in Figure 2. This approach consists of a mix of mid- and high-fidelity approaches to predict advanced liner acoustic performance on a component basis (i.e., single liner sub-element) or within a system (such as a duct or engine nacelle). The primary design path that was used for Task 1 is highlighted in Figure 2 (a dashed black line encircles the design path) and consists of a two-step approach. In the first step, FE simulations of novel liner topologies are performed to predict the acoustic impedance, using a virtual NIT. In the second step, the acoustic impedance is used as a boundary condition in a virtual representation of the NASA GFIT facility for a 16-inch-long liner section. The NASA GFIT facility geometry was selected, as this experimental facility will be used to validate acoustic liner performance in the presence of a grazing flow and sound source. Note that any duct geometry with known source and flow conditions can be utilized within this workflow. The insertion loss (sound power reduction due to the liner) is determined from this simulation as the primary metric to assess liner performance and to down-select concepts for testing at NASA, to be performed in Task 3. This design path was used in Task 2 for refined analysis of advanced liner concepts and concept screening. In Task 1, and as further described below, initial screening of novel acoustic liner concepts was performed by using the high-fidelity LBM-based NIT simulation setup shown in Figure 2. This approach has the advantage that it does not rely on any liner acoustic models, but instead, the exact liner geometry is considered in the analysis and the acoustic performance is determined by using the equivalence of simulating the full Navier–Stokes fluid flow equations. This approach allows us to study the effect of small geometry details on acoustic losses and is suitable for studying novel structures for which the acoustic performance is unknown and for which the acoustic loss mechanisms must be accurately predicted. This approach is more computationally intensive and is therefore not well-suited for design studies, but is more appropriate for exploratory studies. Hence, this approach is used in Task 1, followed by the design approach outlined above for Task 2.

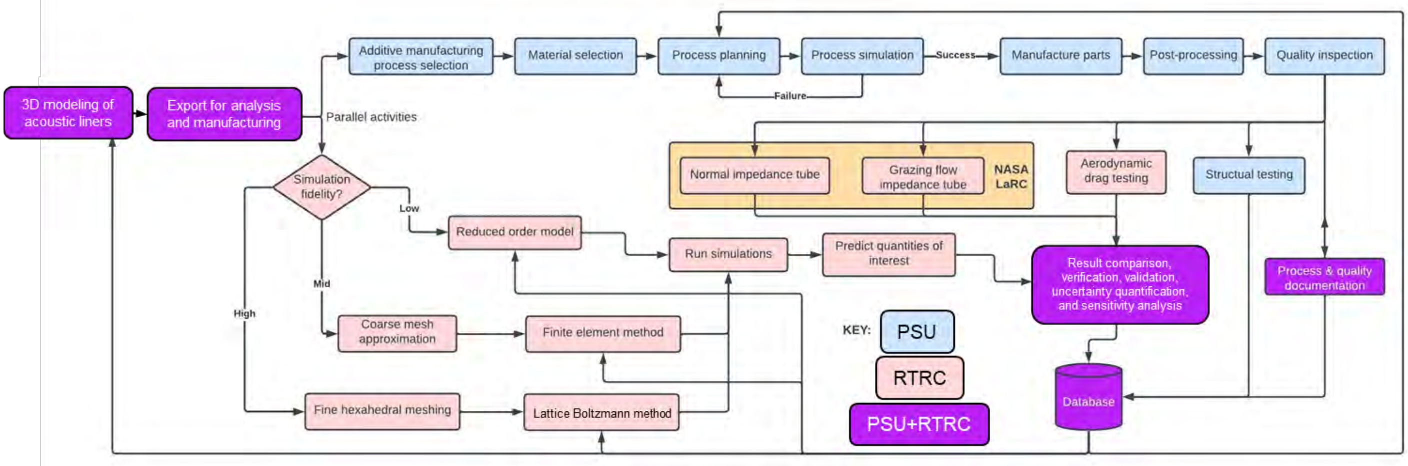

Figure 1. Rapid acoustic liner development methodology. LaRC: Langley Research Center; PSU: The Pennsylvania State University; RTRC: Raytheon Technologies Research Center.

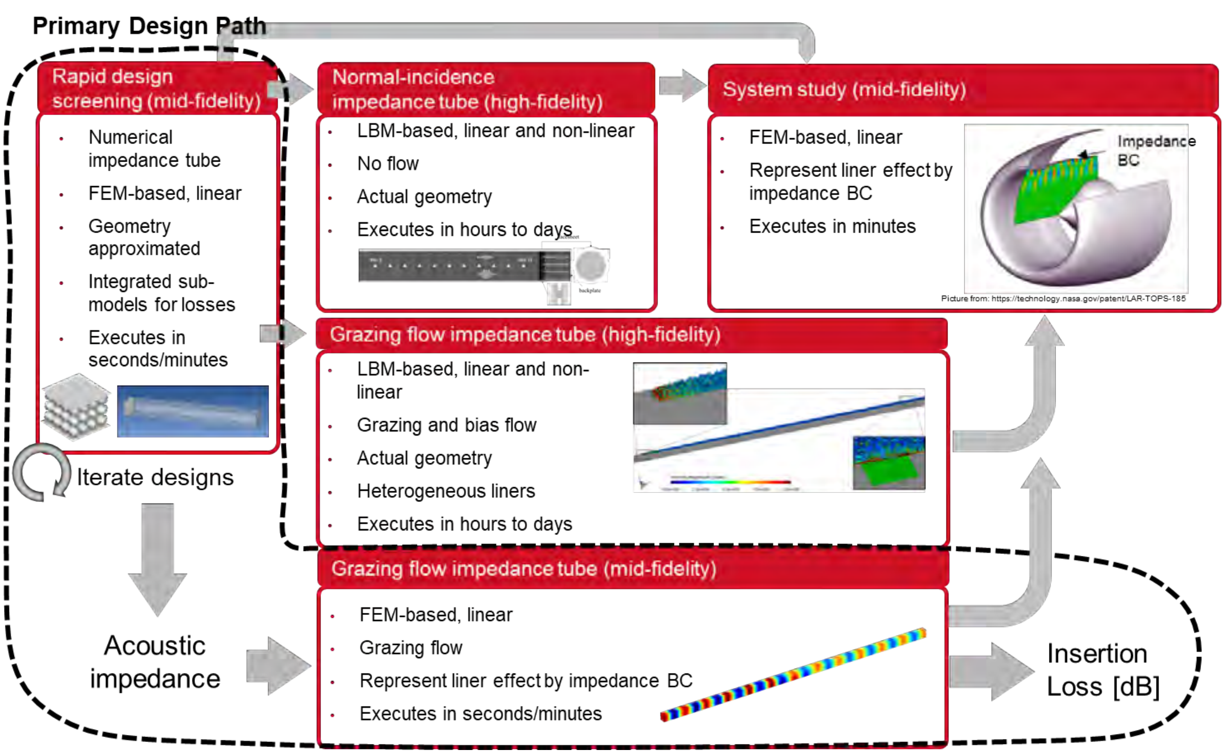

Figure 2. Multi-fidelity modeling and analysis capabilities used for complex acoustic liner design screening. BC: boundary condition; FEM: finite element method; LBM: lattice Boltzmann method.

Reference liner definition and experiments
To validate current prediction models and to establish a baseline for manufacturing and RTRC/PSU test-facility cross-comparisons, a set of single-degree-of-freedom (SDOF) liners was chosen from the literature (Howerton, 2017). The design and performance details of those liners were provided by NASA LaRC. PSU fabricated round and square samples of the AE01 liner, as shown in Figure 3. These test specimens were produced using a Formlabs Form3L SLA resin printer in Grey Pro resin with a layer height of 50 μm and a zero inclination angle, arranged so as to avoid the laser seamline, which causes degradation of small geometries. The specimens were then cleaned per the manufacturer's instructions but were not subject to any additional post-processing. These samples were then tested in the NITs at RTRC and PSU. Additional details on the equipment and methods used during NIT testing can be found in the description of Task 3.

(a) RTRC NIT sample 1 (D = 100 mm)

(b) RTRC NIT sample 2 (D = 29 mm)

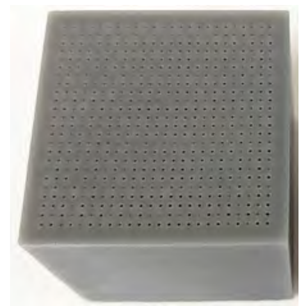

(c) PSU and LaRC NIT sample (L = 50.8 mm)

Figure 3. Initial 3D-printed polymer samples for normal impedance tube (NIT) testing at The Pennsylvania State University (PSU) and Raytheon Technologies Research Center (RTRC). LaRC: Langley Research Center.

Table 1. Corresponding dimensions of initial 3D-printed test samples.

Sample Type	Facesheet Thickness	Facesheet Hole Diameter	Percent Open Area	Liner Core Depth	Outside Core Wall Thickness
LxL square	0.762 mm	0.762 mm	10.18%	51.9 mm	2.5 mm
D=29 mm	0.762 mm	0.762 mm	10.08%	51.9 mm	2.5 mm
D=100 mm	0.762 mm	0.762 mm	10.02%	51.9 mm	2.5 mm

RTRC performed predictions of the liner sample using the high-fidelity LBM simulation approach discussed above and compared those predictions with impedance tube test data. Two different types of simulations were performed: simulations with the as-designed liner and simulations with the as-printed liner. The as-printed geometry was obtained from an x-ray computed tomography (CT) scan via geometry recreation. The as-printed liner was found to deviate slightly from the as-designed liner, as shown in Figure 4. The orifice shapes were rounded compared with the sharp-edged design, and the effective hole diameter and facesheet thickness deviated as well, due to underexposure of the material and shrinkage during post-processing. These differences had a noticeable impact on the acoustic performance, as shown in Figure 4, where the as-designed predictions deviate from the test data. The test data in this figure were obtained from the 29-mm-diameter RTRC NIT.

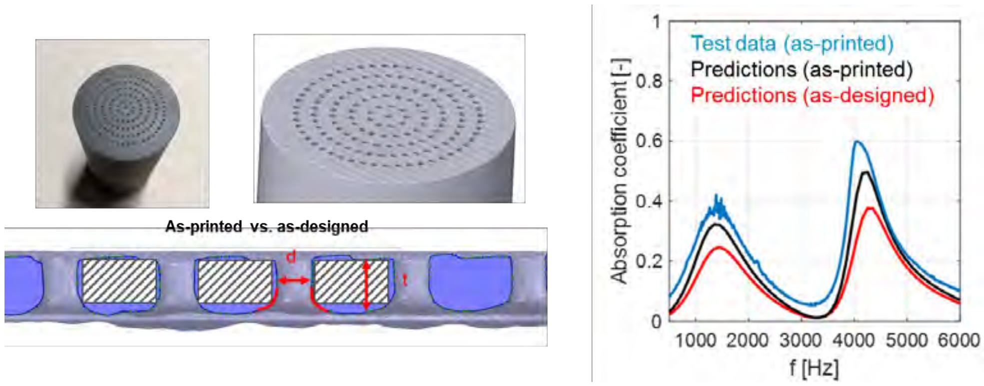

Figure 4. Difference between as-designed and as-printed liner geometry and resulting acoustic performance.

Repeating the simulations with the as-printed geometry 5howed a much closer agreement with the test data, largely closing the "modeling gap." Thus, whereas the as-printed designs deviate from the as-designed liner, it is possible to account for such deviations in the design and manufacturing processes once a quantitative relationship has been established. In addition, this comparison demonstrates how the high-fidelity LBM simulation tool can capture these effects and can ultimately be used to improve the mid-fidelity design tools. The overall agreement between predictions and test data was found to be satisfactory, thus providing the confidence needed to move to the next step of studying more advanced liner concepts with novel backing structures using the high-fidelity LBM approach.

Based on the deviations and defects observed in the first set of AE01 liner samples, adjustments were made to the process settings and materials to minimize future issues. To validate the new manufacturing approach, another set of AE01 liner samples was manufactured and inspected by optical profilometry (OP), which is a rapid, nondestructive, noncontact surface measurement technique (see Figure 5). The primary data outputs of OP include dimensions, surface roughness, and high-resolution images. If needed, these data can be leveraged for additional process improvement or for calculating design correction values.

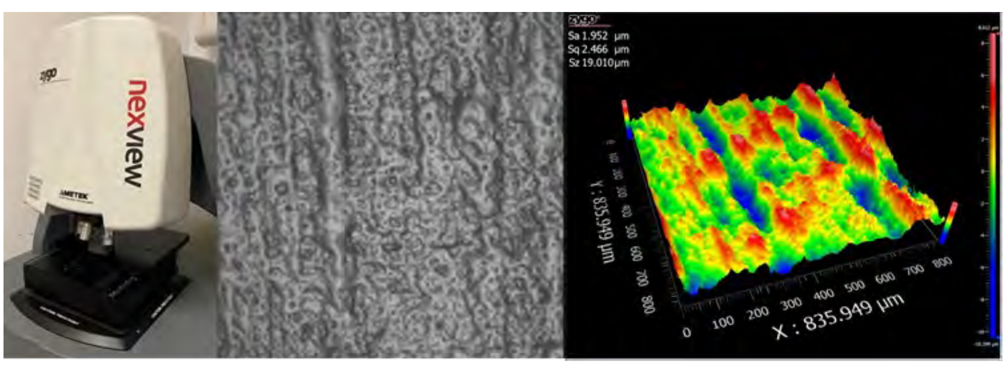

Figure 5. AE01 images and surface roughness measurements acquired with the Zygo Nexview optical profilometry instrument.

To determine whether the new process settings addressed the issue of facesheet hole shrinkage, high-resolution OP images were analyzed with ImageJ, an open-source image-processing software from the National Institutes of Health. Using the particle analysis module, an average hole diameter deviation was determined for each facesheet hole using a co-centric ellipse-fitting approach. Most deviation values fell within the expected tolerance of ±30 µm. The resulting distribution is shown in Figure 6. Significant outliers were typically a result of misalignment between the facesheet holes and the honeycomb core underneath. Ultimately, we determined that it was acceptable to proceed with this manufacturing configuration without using design correction values.

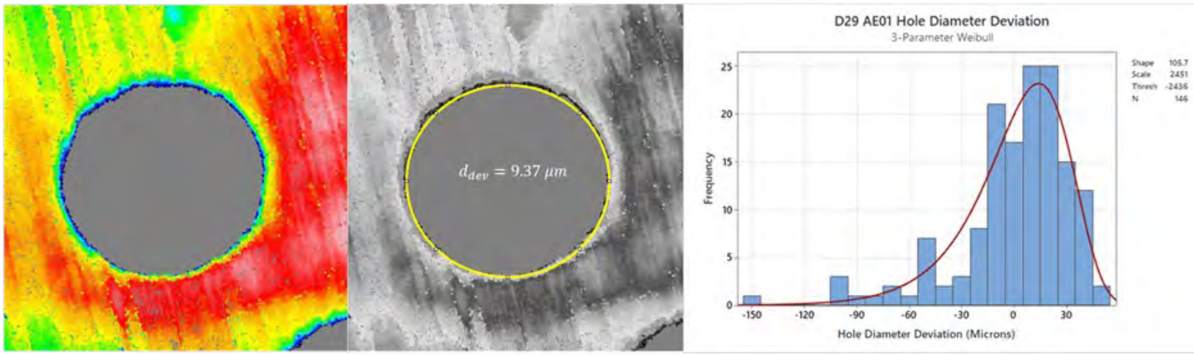

Figure 6. Distribution of facesheet hole diameter deviation.

Evaluation of novel liner backing structures

Triply periodic minimal surfaces (TPMSs) are mathematically well-defined periodic non-self-intersecting surfaces that partition the available volume into two intertwined congruent labyrinth structures. The surfaces represent highly flexible, adaptable, and versatile building blocks for generating more complex structures for material design. Because of the well-defined mathematical nature of these surfaces, one has extensive control over the structures that can be built by manipulating the equations and combining different surfaces. A selection of candidate TPMSs was considered in Task 1, and their potential as novel acoustic liner backing structures was evaluated. MATLAB and the computer-aided design (CAD) software package nTopology were used for geometry generation. The TPMS-based lattice structures shown in Figure 7 were screened for acoustic performance in the absence of grazing flow. The normal incidence acoustic absorption was determined for the structures themselves and in combination with a facesheet.

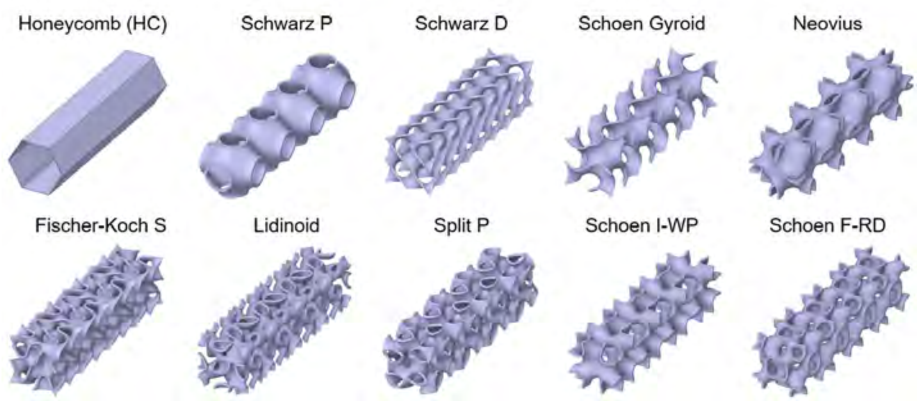

Figure 7. Selected triply periodic minimal surfaces used for performance studies of novel acoustic liners.

In practice, all liners will most likely need a facesheet; otherwise, the drag from flow over the liner would become prohibitvely large. The facesheet also adds further design parameters for tuning the liner acoustic performance, including the facesheet thickness, hole size and distribution (and alignment with the underlying core structure), and total percent open area (POA). The AE01 reference liner facesheet was chosen in conjuction with the TPMS cores. Figure 8 shows simulation results for four of the nine studied surfaces.

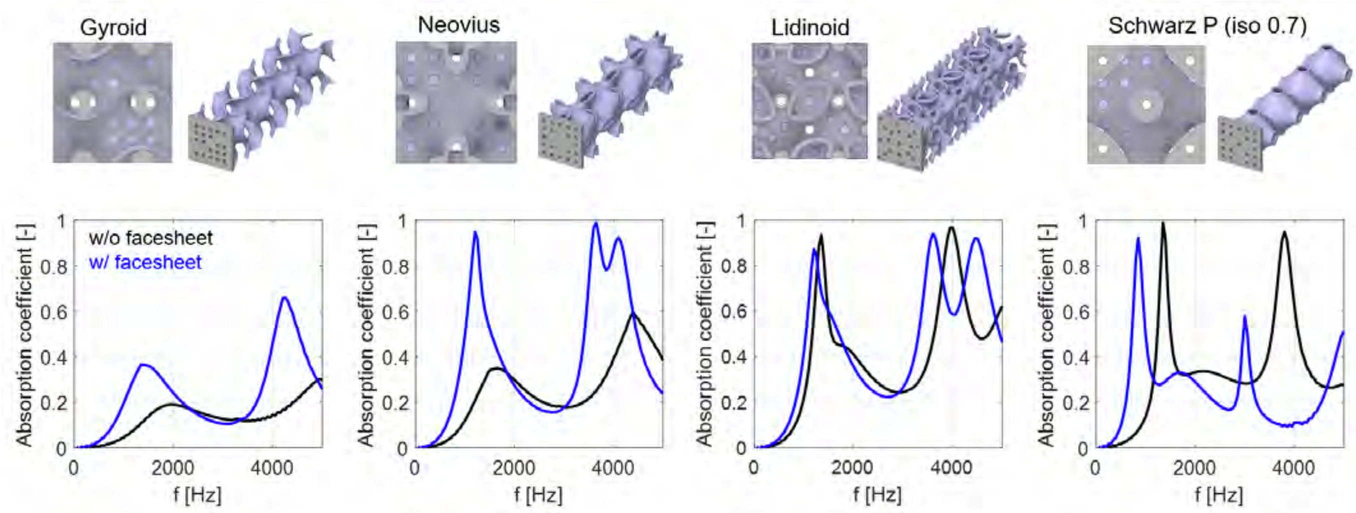

Figure 8. Predicted acoustic performance of advanced liner cores with and without the AE01reference liner facesheet.

As expected, the facesheet can have a pronounced impact on acoustic performance and must therefore be included in the analysis. However, even without a facesheet, all of the TPMS cores show pronounced acoustic absorption behavior in two separate frequency regions. These regions are related to the two different parallel paths of the acoustic wave as it passess through each TPMS: in all TPMS structures considered, the available volume is partitioned into two seperate regions. Some TPMS geometries inherently show a stronger response than others. For example, the Gyroid structure without a facesheet has a rather broadband response and low acoustic absorption, whereas the Lidinoid or Schwarz P surfaces have very pronounced and sharp peaks with high acoustic absorption, even in the absense of a facesheet. This trend is related to the underlying geometry, which consists of regions of large volume connected to neighboring regions through narrow constrictions. The Schwarz P structure is the simplest, with large volumes connected to its neighbors through narrow necks along all Cartesian directions, whereas the lidinoid structure has smaller volumes connected to each other through off-axis narrow constrictions. From a fluid mechanics perspective, these surfaces act as coupled Helmholtz resonators. Therefore, through geometry design changes, it should be possible to tune the resonance frequencies so that a desired acoustic absorption behavior (peak absorption and target frequency range) can be obtained.

To further illustrate the acoustic design choices, Figure 9 compares the acoustic performance of the Lidinoid, Neovius, and Schwarz P surfaces with a perforated facesheet. Although the underlying geometry is very different in all three cases and the internal acoustic response appears different (as shown in the contour plots), the overall acoustic performance in terms of absorption behavior is very similar for all three surfaces. This finding illustrates that different TPMS-based liners can be used to achieve the same acoustic performance. While, in principle, it is possible to proceed with designs of all of the TPMS-based liner candidates, it appears that the Schwarz P structure is geometrically the simplest of all of the surfaces while having sufficient degrees of freedom for design tuning through bulb volume and neck length and size. However, the other surfaces offer similar abilities for design tuning. Additional information is needed to down-select a suitable TPMS candidate for the advanced liner design to be performed under Task 2. For this purpose, additional requirements must be considered, related to the weight of the acoustic liner.

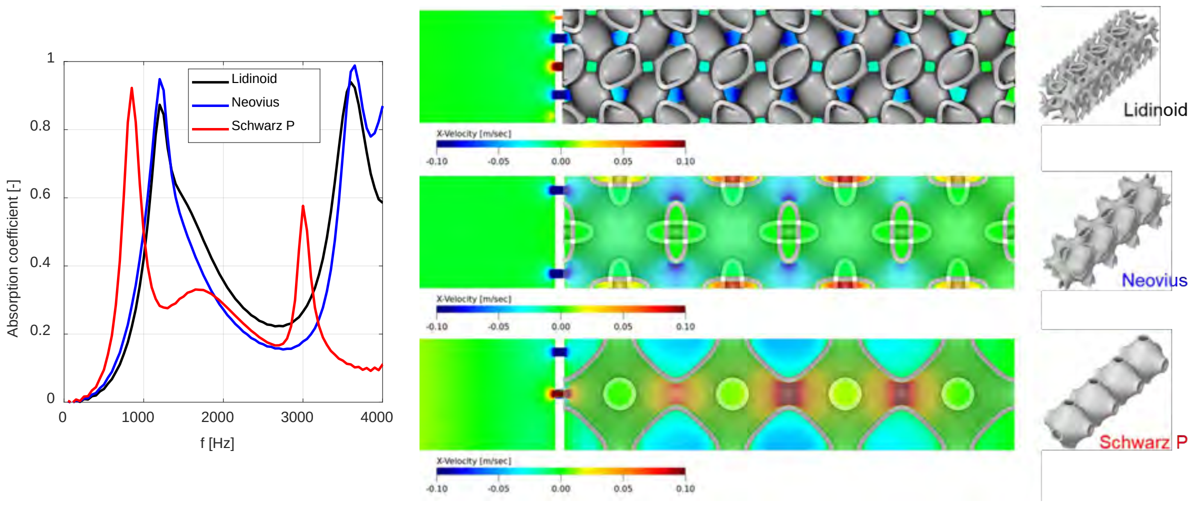

Figure 9. Predicted normal incidence acoustic absorption for advanced liners with selected triply periodic minimal surface cores.

In addition to assessing the acoustic performance of TPMS-based liners, the team performed a weight impact study, in which the surface area per unit volume was computed for each TPMS under consideration (a selection of TPMS candidates is shown in Figure 7) and compared with that of a standard honeycomb core. The goal was to obtain an advanced liner that performs better than a SDOF liner with a honeycomb core, with a reduced footprint and comparable or reduced weight. The results for a few select TPMS structures are shown in Figure 10.

The contour maps in Figure 10 show ratios of wall thickness (with respect to the honeycomb) on the horizontal axis and ratios of liner volume on the vertical axis. The contours show the weight impact relative to a honeycomb core. Contour regions in blue indicate a weight reduction compared with a standard honeycomb liner, and contours in red show a weight increase. The yellow circle shows the reference location for a liner with equal wall thickness and liner volume (depth) compared with a SDOF honeycomb core liner. For both Schwarz P and Neovius surfaces, the respective contour plots show a potential weight reduction, while the liner with a Lidinoid core would result in a weight increase. Similar maps were created for other TPMSs.

Based on these results, it was found that the Schwarz P surface provides the best surface candidate for novel liner cores, as it has the lowest surface area of all surfaces studied. In combination with its acoustic performance, the Schwarz P surface was identified as the leading candidate, as it has the lowest surface area of all TPMSs, while providing sufficient degrees of freedom to tune the structure for acoustic performance, as noted previously. Thus, we decided to proceed with Schwarz-P-based liner designs for refined analysis under Task 2.

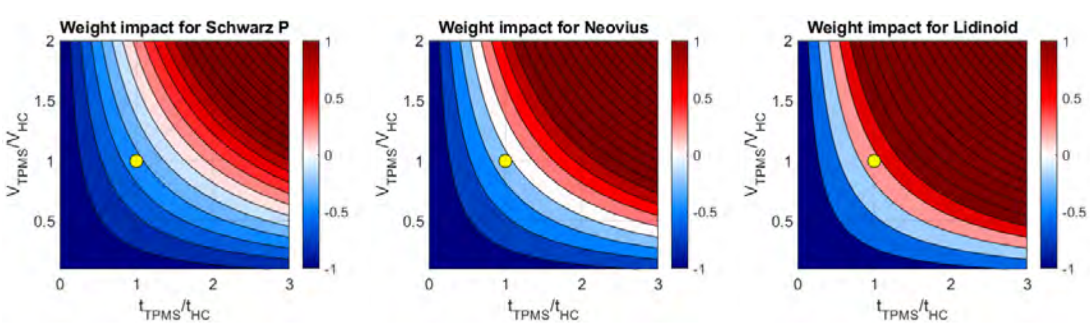

Figure 10. Weight impact maps for selected triply periodic minimal surfaces (TPMSs). HC: honeycomb core.

Milestone(s)

1. Demonstrated acoustic liner design and analysis using multi-fidelity modeling framework.
2. Fabricated baseline acoustic liners and TPMS-based lattice structures for experimental testing.
3. Identified Schwarz P lattice structure as best candidate for novel liner cores

Major Accomplishments

1. Designed and analyzed lattice-based acoustic liners using advanced software tools.
2. Performed rapid, iterative prototyping and testing to identify a promising acoustic liner design.
3. Conducted preliminary assessment of manufacturability variation within 3D printed test samples.

Publications

We plan to prepare 2–3 conference publications once experimental evaluation is complete. These publications will focus on the rapid design and analysis framework using 3D printing and modeling, analysis, and comparison with NIT test results. We will target both American Institute of Aeronautics and Astronautics (AIAA) technical conferences and AM conferences; accepted conference papers will be revised, updated, and submitted to journals as appropriate.

Outreach Efforts

None.

Awards

None.

Student Involvement

Two graduate students are involved in this research: (1) Andy Swanson, a graduate student working toward his MS in PSU's Additive Manufacturing & Design Graduate Program, and (2) Michael Geuy, a graduate student working toward his PhD in Mechanical Engineering. Andy is focusing on the rapid design and analysis framework; Michael is focusing on fabrication and manufacturing analysis.

Plans for Next Period

By the end of Year 1, the proposed framework will have been verified and validated using both 3D-printed baseline geometries and more complex liner designs derived from promising TPMS structures. Year 2 will focus on expanding the development methodology to include detailed manufacturability assessments of 3D-printed liner structures and detailed assessments of aerodynamic performance (targeting low drag).

Reference

Howerton, B. M. & Jones, M. G. (2017, June 5). A conventional liner acoustic/drag interaction benchmark database. *23rd AIAA/CEAS Aeroacoustics Conference*. 23rd AIAA/CEAS Aeroacoustics Conference, Denver, CO. https://doi.org/10.2514/6.2017-4190

Task 2 - Detailed Design and Additive Fabrication of Novel Liner Solutions

PSU and RTRC contributed to this task.

Objective

The goal of this task is to finalize the design and to additively manufacture novel acoustic liner solutions for testing and evaluation of a few select concepts.

Research Approach

The liner design approach employed in this study consisted of two steps, as described in Task 1 (see Figure 1). The first step is the prediction of the acoustic impedance based on a virtual NIT through FE modeling. In the second step, the predicted acoustic impedance is applied as an acoustic boundary condition representing the liner in a virtual grazing flow test model (which emulates NASA's grazing flow test setup) to predict the insertion loss and to down-select leading concepts for acoustic testing. The following sections explain this two-step process in more detail.

Prediction of normal incident liner impedance
Figure 11 shows the virtual NIT setup based on ACTRAN, a general-purpose acoustic modeling FE software.

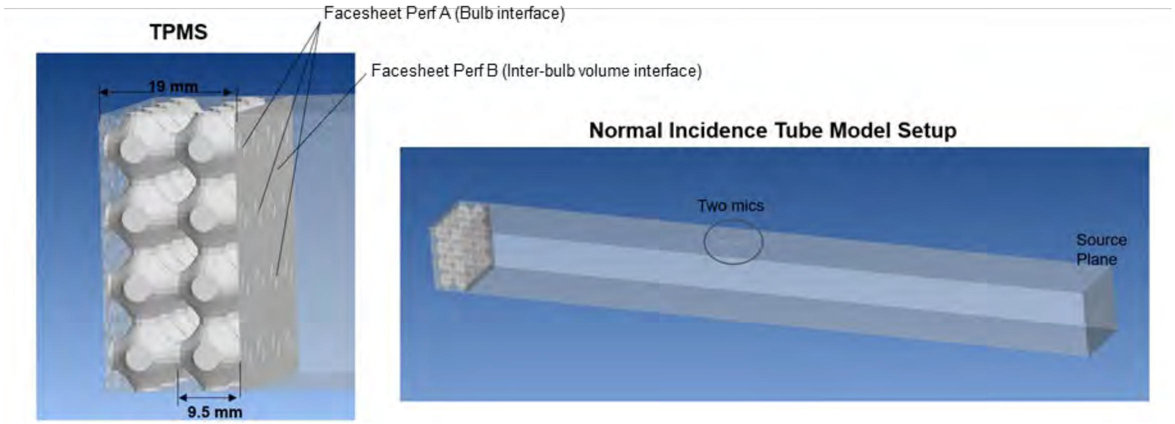

Figure 11. Liner acoustic impedance prediction based on a virtual impedance tube model setup in ACTRAN. The liner coupon model is based on a Schwarz P triply periodic minimal surface design with two bulb layers with front perforated sheets incorporating the transfer acoustic impedance calculated from a semi-analytical perforate model from the literature.

The model simulates a waveguide tube with an acoustic excitation source (i.e., a speaker) located at one end and an acoustic liner model situated at the other end. Two virtual microphones are used to measure the incident and reflected sound waves, which in turn are used to calculate the absorption coefficient and the acoustic impedance of the liner. The liner in Figure 11 is based on the Schwarz P TPMS geometry with a perforated facesheet located at the front of the liner.

In this model, the geometry of the Schwarz P TPMS is modeled with an FE mesh, while the front perforated facesheet is represented by the pre-calculated equivalent transfer impedance, based on an industry-standard semi-analytical perforate model, the Goodrich model (Yu, et al., 2008). The Goodrich model takes into account the effect of grazing flow across the perforated facesheet. Figure 12 shows the effect of the grazing flow on the liner acoustic impedance and the absorption coefficient for a Mach number, M, range of 0 (no flow) to 0.5 for an advanced acoustic liner with a Schwarz P TPMS core.

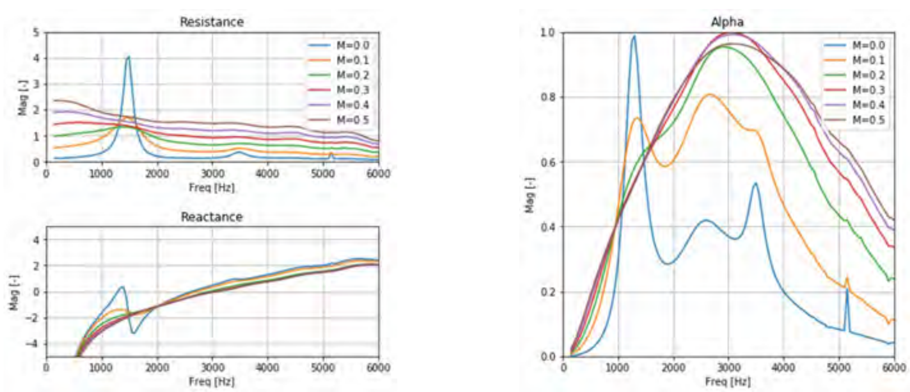

(a) Acoustic impedence (b) Normal sound absorption

Figure 12. Predicted effect of grazing flow on a Schwarz P triply periodic minimal surface liner before redesign for a grazing flow fat M = 0–0.5.

As shown in Figure 12(a), the presence of grazing flow significantly alters the acoustic performance, particularly the acoustic resistance, which tends to increase with flow Mach number. The absorption plot in Figure 12(b) shows that the absorption performance at relatively low Mach numbers (M < 0.1) consists of multiple absorption peaks, starting with a prominent peak at approximately 1200 Hz. At higher Mach numbers (M > 0.2), these multi-peak characteristics disappear, and instead, the absorption is dominated by a single peak at a relatively high frequency of 3000 Hz. Further studies revealed that this result was due to reduced participation of the resonances associated with the Schwarz P bulb cavities caused by an excessive flow-induced resistance increase for the front perforated facesheet facing the bulb cavities. This prompted a redesign of the geometry parameters (hole diameter [d] and POA) of the bulb entrance perforated facesheet. Figure 13(a) shows the flow-dependent acoustic resistance term (labeled "Zgraz" in the figure) as a function of the two performance parameters. As shown in the figure, this flow-dependent resistance can be further reduced by increasing the POA while reducing the hole diameter, d.

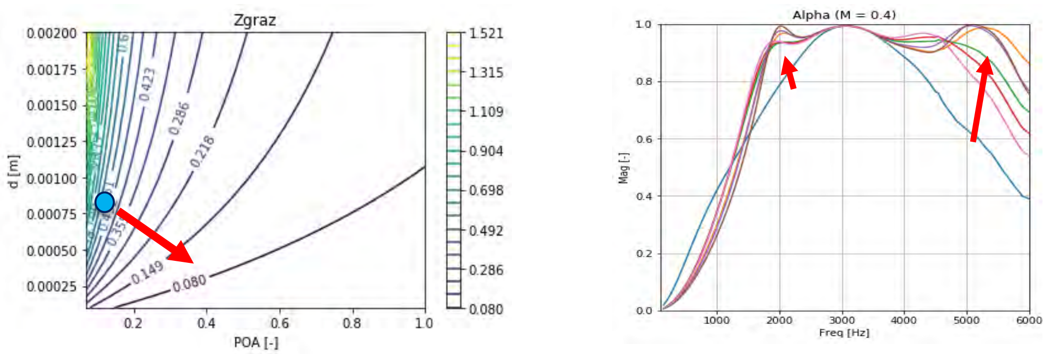

(a) (b)

Figure 13. Tuning the triply periodic minimal surface liner design parameters for a higher-Mach-number flow. (a) Flow-dependent acoustic resistance term (Zgraz) as a function of bulb entrance perforate diameter, d, and percent open area, POA. (b) Liner absorption with retuned bulb perforated facesheet parameters (absorption before retuning is shown by the blue curve).

Figure 13(b) shows the absorption performance of the Schwarz P TPMS liner at M = 0.4 for several different designs of the bulb entrance perforated facesheet. As shown in the figure, by retuning the bulb entrance perforated facesheet parameters, one can adjust the acoustic resistance and recover the bulb resonance contributions, thus achieving the desired multiple-resonance-peak absorption characteristics (which broadens the frequency bandwidth).

This investigation was critical to the design and study of advanced Schwarz-P-based liners. Numerous designs were investigated, targeting low-frequency tonal noise control (relevant to blade-pass frequencies and higher harmonics) as well as broadband performance. For each advanced liner design candidate, the acoustic impedance was determined via the simulation approach described above and then further analyzed in a virtual grazing flow simulation before the concepts were down-selected for printing and testing, as described next.

Prediction of grazing flow test insertion loss

The virtual impedance tube model in the previous step provides a means for screening multiple designs of Schwarz P TPMS-based liners. The next step is to predict the performance of the candidate designs in a grazing flow test setup that is closer to a realistic engine nacelle liner application. Figure 14 shows the ACTRAN simulation model that emulates NASA's grazing flow test setup.

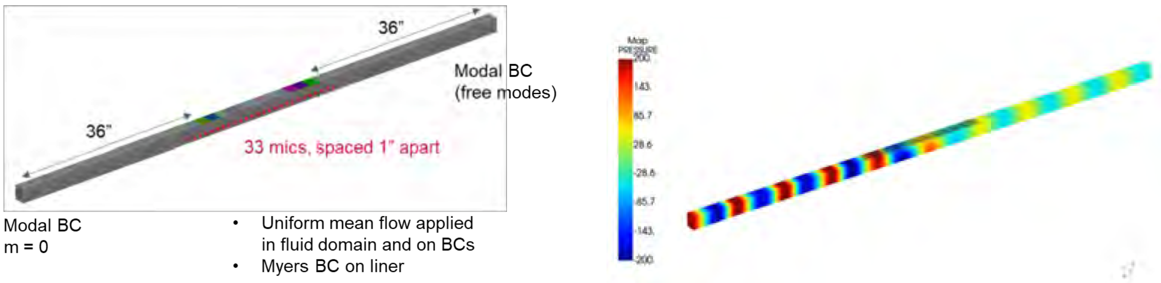

(a) Model setup

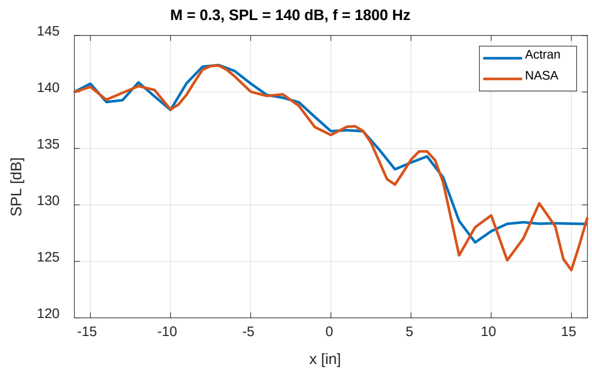

(b) Sound pressure level (SPL) as a function of axial position

Figure 14. Grazing flow test model for predicting liner attenuation performance. (a) The virtual glazing flow test model setup and (b) model vs. NASA test data for a reference single-degree-of-freedom liner. BC: boundary condition.

Unlike the NIT, which measures the acoustic liner performance for sound incident on the liner at a normal angle, the grazing flow setup measures the liner performance with respect to the sound propagating across the liner surface in the presence of air flow at engine-relevant Mach numbers. The grazing flow test tube model image shows the sound-propagating tube with a liner section in the middle, which is represented as a boundary condition with its frequency-dependent liner acoustic impedance values (obtained from the NIT model of the earlier step). This model was first validated with published attenuation performance data for SDOF liners. Figure 14(b) shows that the model-predicted sound pressure level (SPL) attenuation as a function of axial location compares well with that of the NASA data. Thus, the setup can be used reliably to study advanced liner performance.

Figure 15 shows the model-predicted insertion loss performance of two Schwarz P liner designs (three bulb layers, total depth of 1 inch) that were down-selected for the planned grazing flow testing at the NASA facility.

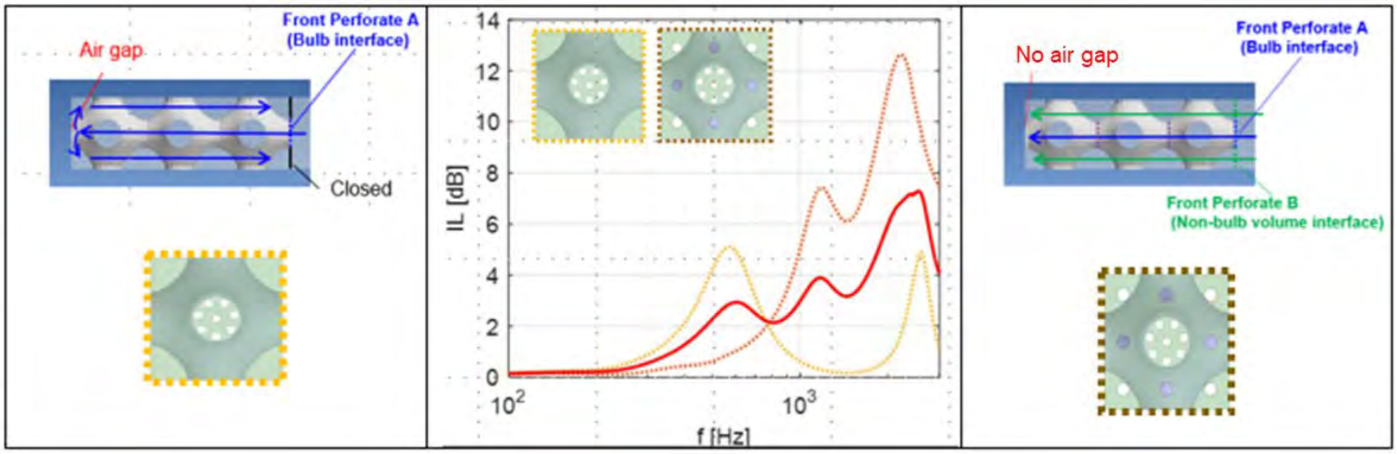

Figure 15. Predicted insertion loss (IL) performance of Schwartz P triply periodic minimal surface liner designs for planned grazing flow impedance testing at the NASA facility.

There are two variations of the Schwarz P TPMS-based liner designs with different target frequency ranges. One design targets 1–3 kHz while the other design targets the low-frequency range near 600 Hz. These liners have been designed specifically for testing with NASA's grazing flow test facility, which covers the frequency range of 400–3000 Hz.

Milestone(s)

1. Detailed acoustic evaluation of acoustic liner designs based on Schwarz P triply periodic minimal surface.
2. Identified two variations of Schwarz P lattice structure for noise attenuation in two different frequency ranges.

Major Accomplishments

1. Analyzed geometric variations of Schwarz P triply periodic minimal surface to optimize acoustic attenuation.
2. Predicted insertion loss of Schwarz P acoustic liner for grazing flow impedance testing.

Publications

We plan to prepare 1-2 conference publications once experimental evaluation is complete. These publications will discuss fine-tuning of the Schwarz P liner designs and modeling, analysis, and comparison with GFIT test results. We will target American Institute of Aeronautics and Astronautics (AIAA) technical conferences; accepted conference papers will be revised, updated, and submitted to journals as appropriate.

Outreach Efforts

None.

Awards

None.

Student Involvement

None.

Plans for Next Period

Year 2 will fabricate acoustic liner samples for grazing flow impedance testing and compare experimental results to predicted values. Analysis and simulation models will be refined and updated as needed.

Reference

Yu J, Ruiz, M. & Kwan, H.W. (2008, May) Validation of Goodrich Perforate Liner Impedance Model Using NASA Langley Test Data, *14th AIAA/CEAS Aeroacoustics Conference*, Vancouver, British Columbia Canada, AIAA-2008-2930.

Task 3 - Acoustic Evaluation of Additively Manufactured Novel Liners

Objective

The goal of Task 3 is to perform an acoustic evaluation of the additively manufactured novel liner designs generated in Tasks 1 and 2, leveraging multiple experimental testing capabilities at PSU, RTRC, and NASA LaRC.

Research Approach

Currently, two different experimental methods are being employed to evaluate the acoustic performance of different liner concepts, as shown in the development methodology in Figure 1: NIT and GFIT testing. A summary of the acoustic testing capabilities available at PSU, RTRC, and NASA LaRC for experimental evaluation is given in Table 2. Images of the NITs and GFIT facilities listed in Table 2 are shown in Figures 16 and 20, respectively.

Table 2. Summary of capabilities available at The Pennsylvania State University (PSU), Raytheon Technologies Research Center (RTRC), and NASA Langley Research Center (LaRC) for experimental testing. GFIT: grazing flow impedance tube; NIT: normal impedance tube; SPL: sound pressure level.

Acoustic Testing Capabilities Summary		Location	Sample Dimensions	Source Type(s)	Frequency Range	Maximum SPL	Centerline Mach Number
NIT	Brüel & Kjær Impedance Tube Kit Type 4206 (Large Sample Config)	RTRC	Diameter = 100 mm Height ≤ 400 mm	Broadband	500 Hz to 6.4 kHz	140 dB	0.0
	Brüel & Kjær Impedance Tube Kit Type 4206 (Small Sample Config)		Diameter = 29 mm Height ≤ 200 mm		50 Hz to 1.6 kHz		0.0
	In-House-Developed NASA Langley Specification Impedance Tube	PSU	Length = 2 in Width = 2 in Height ≤ 8.5 in	Stepped Sine Swept Sine Broadband	377 Hz to 3.4 kHz	146 dB (Broadband)	0.0
	Six-Driver High-Intensity Impedance Tube	NASA LaRC	Length = 2 in Width = 2 in Height ≤ 24 in	Stepped Sine Swept Sine Broadband	400 Hz to 3.0 kHz	155 dB (Stepped Sine) 145 dB (Swept Sine) 140 dB (Broadband)	0.0
GFIT	In-House-Developed Grazing Flow Impedance Tube	RTRC	Length = 2 in Width = 16.375 in Height ≤ 5 in	Stepped Sine Broadband	500 Hz to 6.5 kHz	160 dB	0.0–0.65
	In-House-Developed Grazing Flow Impedance Tube	NASA LaRC	Length = 2 in Width = 2–24 in Height ≤ 3 in	Stepped Sine Broadband	400 Hz to 3.0 kHz	155 dB (Stepped Sine) 145 dB (Swept Sine)	0.0–0.6

As previously mentioned, testing with NITs was primarily used to inform computational modeling and to screen out design concepts. While many different NIT configurations exist, the NITs used in this project (see Figure 16) have been configured to perform measurements using the two-microphone method from ASTM standard E1050-19. This standard calls for one or more sound sources (loudspeakers/compression drivers) to be fixed to one end of the NIT waveguide and for the sample of interest to be placed at the other end. The source then generates sound waves that travel down the tube toward the sample. By measuring the acoustic pressure over time with two stationary microphones, one can calculate the sample's absorption coefficient and acoustic impedance as a function of frequency using the signal processing algorithm explained in the ASTM testing standard. Typically, several measurements are made for a single sample to ensure consistency. In addition, the sound source type and SPL levels are varied so that non-linear effects can be evaluated.

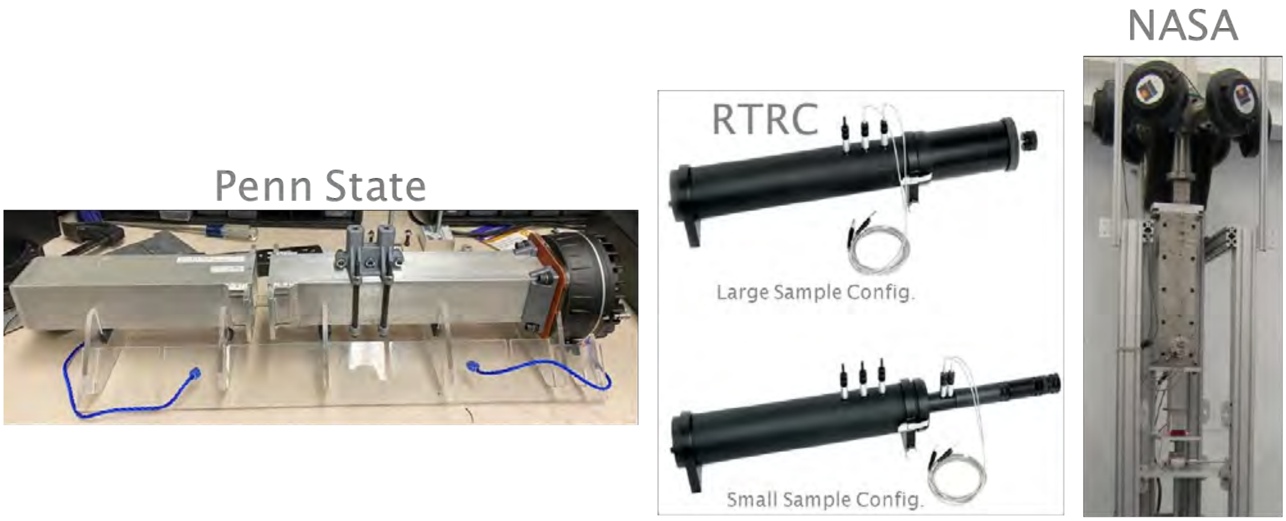

Figure 16. Normal impedance tubes found at The Pennsylvania State University, Raytheon Technologies Research Center (RTRC), and NASA Langley Research Center.

A few actions must be carried out before and during testing to ensure the quality of the NIT measurements. One of the most important preliminary steps is calibrating both microphones using an acoustic sound calibration device. Calibration ensures that the microphones are working correctly and making accurate measurements. Another important initial step is to validate the NIT measurements by testing a sample with a known absorption coefficient and comparing that with the observed results. For example, as shown in Figure 17, the PSU NIT was validated by testing a one-inch-thick Hushcloth foam sample and comparing the measured absorption coefficient with data provided by the manufacturer. When testing the samples, it is important to ensure that the sample and tube interfaces fit together correctly so that leakage does not affect the results. Petroleum jelly can be used to seal any gaps that remain after sample placement. Finally, one must also verify the software used to process the data by testing it on datasets with known solutions.

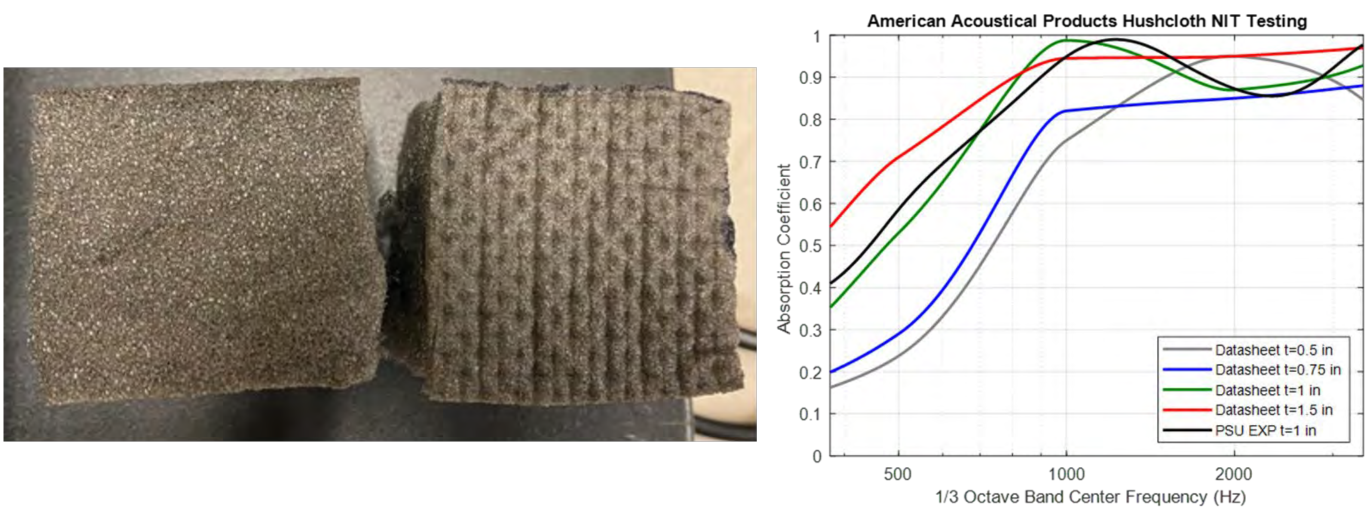

Figure 17. Validation of the normal impedance tube (NIT) at The Pennsylvania State University with Hushcloth foam (comparing black and green curves).

One of the most significant advantages of using a NIT to evaluate samples is speed, which makes this approach an ideal method for testing AM liner samples because of how rapidly prototypes can be produced. This synergy was leveraged at the beginning of the project to test the eight different AM design concepts shown in Figure 18. These designs included several

TPMS-based liners, a stochastic Voronoi foam lattice, an internal labyrinth, and a honeycomb to serve as a baseline. In addition to the different geometries, each design was printed out of thermoplastic polyurethane (TPU) and polylactic acid (PLA) polymers, soft and hard materials, respectively, to determine whether the material had any effect. In total, it took only a few hours to test and process the data from all 16 samples.

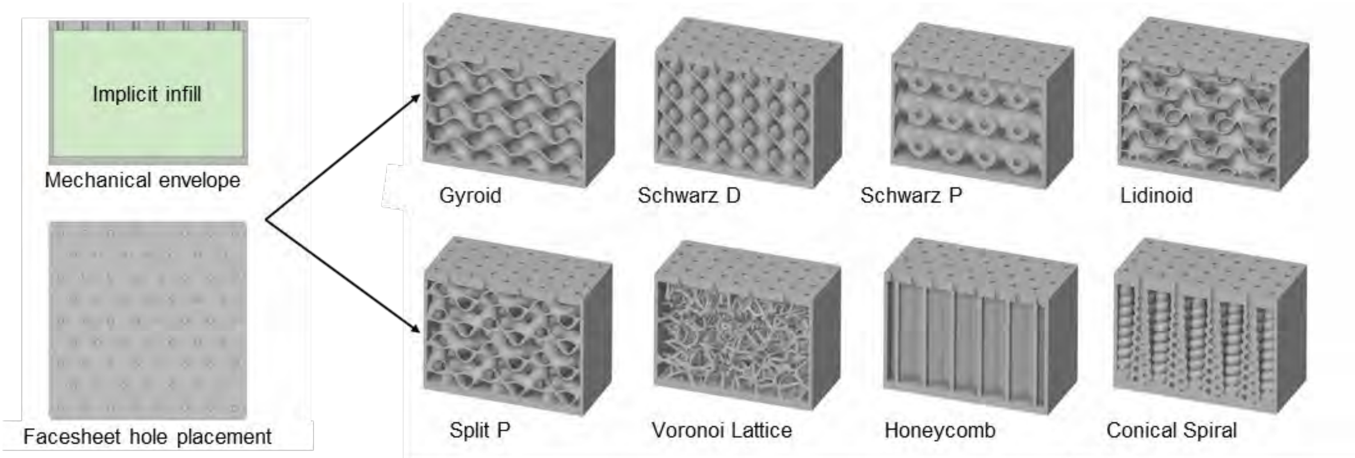

Figure 18. Eight additively manufactured acoustic liner designs evaluated with a normal impedance tube.

The absorption coefficients for the eight different designs and both materials are plotted in Figure 19. In general, the soft TPU and hard PLA performed similarly. However, in some cases, such as the Gyroid design, it is hypothesized that the soft TPU material would allow the facesheet to vibrate, adding to the overall absorption. These results also provided insights into what structures should be further investigated. In particular, the Schwarz P and Lidinoid TPMS surfaces were identified as having potential owing to their dual-degree-of-freedom absorption behavior.

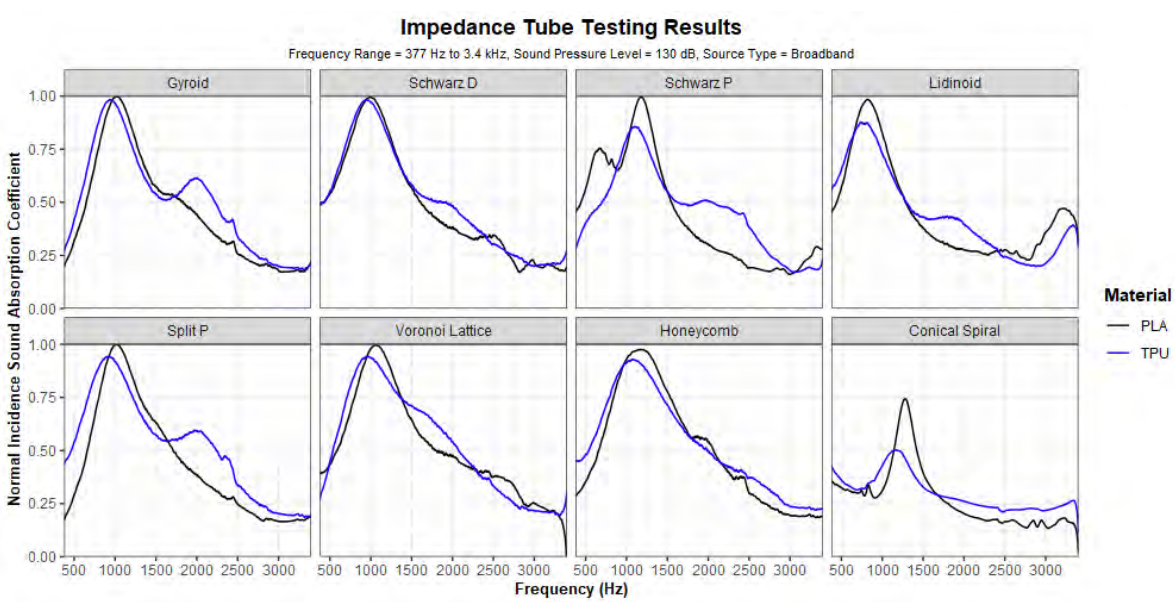

Figure 19. Absorption coefficients of the initial liner designs.

One of the downsides of evaluating liners with NITs is that flow effects are not considered. This presents an issue because, as found in Task 2, a liner's acoustic behavior strongly depends on the grazing flow it experiences. Therefore, when grazing flow effects need to be experimentally evaluated, one of the GFITs shown in Figure 20 is used. By combining acoustic sound sources, a wind tunnel, and several microphone arrays in a single environment, key aeroacoustic performance metrics, such as drag force, acoustic impedance, and insertion losses, can be determined.

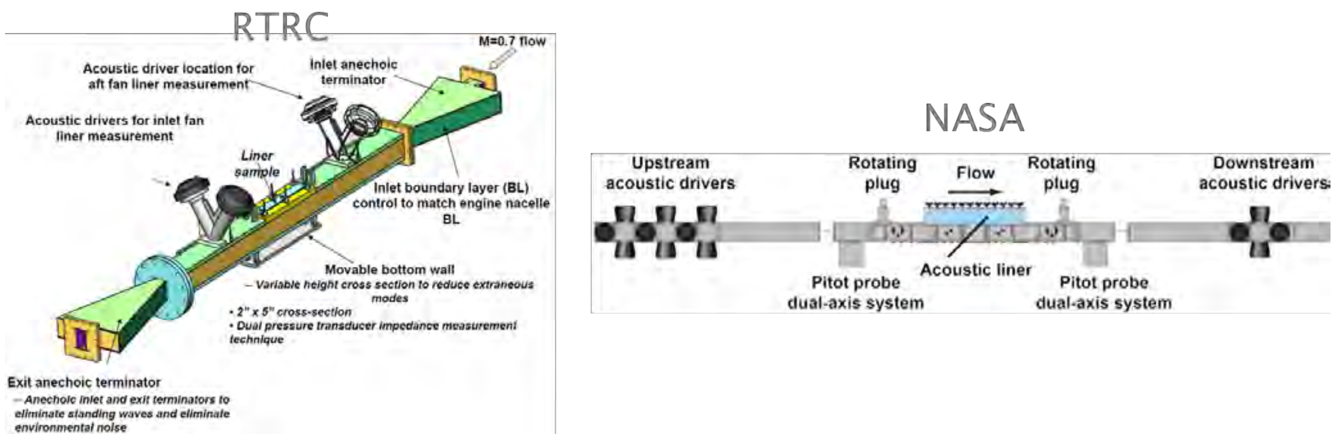

Figure 20. Grazing flow test facilities at RTRC and NASA Langley Research Center.

We are currently in the process of finalizing test samples for GFIT testing. The as-printed geometries will be measured and characterized prior to testing at RTRC. Samples will then be sent to NASA LaRC for testing in their grazing flow facility for comparison. These efforts will be a significant milestone for the project once testing is completed.

Milestone(s)

1. Compiled list of NIT and GFIT experimental facilities at PSU, RTRC, and NASA LaRC.
2. Verified baseline acoustic performance of NIT facilities at PSU and RTRC.

Major Accomplishments

1. Validated NIT evaluation capabilities at PSU and RTRC with baseline testing.
2. Performed experimental testing of multiple TPMS-based acoustic liner designs in PSU NIT facility.

Publications

We plan to prepare 2–3 conference publications once experimental testing is complete.

Outreach Efforts

None.

Awards

None.

Student Involvement

Two graduate students are involved in this research: (1) Andy Swanson, a graduate student working toward his MS in PSU's Additive Manufacturing & Design Graduate Program, and (2) Michael Geuy, a graduate student working toward his PhD in Mechanical Engineering. Andy is focusing on the rapid design and analysis framework; Michael is focusing on fabrication and manufacturing analysis.

Plans for Next Period

Additional testing of acoustic performance and material evaluation for successful manufacturing of the proposed liner concepts and a far-field noise impact study of these novel liner designs will be conducted in Year 2 to assess their merits compared with conventional and other reference liner solutions. The focus in Year 2 will also shift to acoustic liner design for a specific section of the engine, expanding from component-level tradeoffs (e.g., weight, acoustic performance, structural integrity) to subsystem-level tradeoff studies (e.g., weight, cost, drag).